# Updated Conceptual Model of Olkaria Geothermal Field Naivasha, Kenya.

**Joyce Okoo, Ammon Omiti, Kennedy Kamunya and Daniel Saitet**

**Keywords**

*Structures, Alteration, Permeability, Up-flow*

**ABSTRACT**

This paper presents the results of the Olkaria conceptual model update which was carried out in the year 2015 to 2016. In this update, data from different disciplines is analyzed separately before they are jointly visualized in Petrel software. The results of this update are presented first through different discipline reports and thereafter jointly interpreted to update the conceptual model of the system. Olkaria consists of large collapsed caldera thought to be of recent age dominated by thick pyroclastic deposits at surface with rhyolite and trachyte successions at depth. The principle reservoir is dominated by trachytic rocks. The dominant regional structural trend is in the NW-SE strike. Major controls of permeability strike in a generally opposite direction resulting in a complex grid structure. The existence of circular structures both on the outer margins as well as around some major up flow regions is evident.

These structures play an important role either as conduits of colder recharge and therefore barriers or as permeability controls. The recharge structures generally trend north-south with fluids flowing from the north to recharge the system. Six different up flow regions are evident in the area separated by regions of colder incursions thought to be recharge conduits. The existence of these up-flow zones is supported by Cl-ion concentration data and Na/K temperature estimates as well as resistivity data. The up flow regions are located under the EPF, NEPF, DPF, WPF, SEPF and the region of OW-101 (CPF and NWPF). These are well developed mushroom structures that up well close to surface. In this study several extensions to these up flows are discovered with recent drilling activities. These up flows are separated from each other by shallow colder flows that sometimes extend into reservoir depths. These are thought to be regions of colder recharge into the system and are clearly structurally controlled. In some cases these colder incursions up well when they are sufficiently heated up at the top of the mushroom structures.

## 1. INTRODUCTION

### *1.1 General information*

The Olkaria Volcanic complex is located in the Kenya Rift valley (Figure 1), about 120 km from Nairobi. It is bounded to the north by Eburru complex and to the east and south by the Longonot and Suswa volcanoes, respectively. Olkaria geothermal field is divided into smaller sectors

(Figure 2) namely East, Northeast, Southwest, Northwest, Southeast, Domes and Central Olkaria, all relative to the position of the Olkaria volcanic centre and for ease of development. Exploration of the Olkaria geothermal resource started in 1956. Power production started in Olkaria East field in 1981 when the first 15 MWe turbo-generator Unit was commissioned. Currently total installation in Olkaria geothermal field is 675.4 MWe, comprising of Olkaria I: 45 MWe, Olkaria I AU: 150.5 MWe, Olkaria II:105 MWe, Olkaria III: 140 MWe, Olkaria IV: 149.8 MWe (Gudni et al 2016), and 4 MWe Oserian 1 & 2 (Omenda and Simiyu 2015). In addition KenGen has installed 15 well-head plants in Olkaria field with a combined capacity of 81.1 MWe (KenGen 2017)

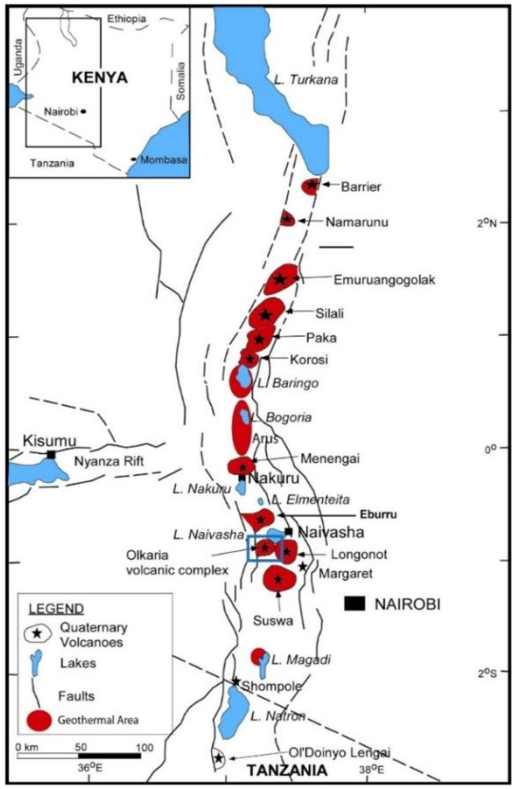


**Figure 1: Map of Kenya showing the location of Olkaria geothermal field and other Quaternary volcanoes along the rift axis (Omenda and Karingithi, 1993)**

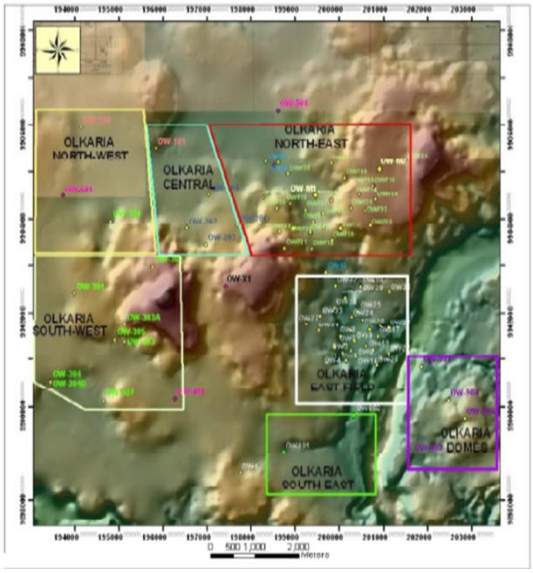


**Figure 2: Sub-sectors of the Greater Olkaria Geothermal Field**

### *1.2 Previous models*

The first published version of the Olkaria conceptual model was presented by SWECO and Virkir (1976). This model included a boiling geothermal reservoir overlain by a steam zone,

capped by tuffaceous caprock and meteoric water percolating down to 1600 m b.s.l. where it was heated to about 320°C. The hot water was then assumed to rise and eventually boil with the steam condensing below the cap rock to sink again in a kind of convective cycle. Ofuona (2002) showed, in his revised model, that the hydrothermal systems of western and eastern Olkaria are clearly separated by the low pressure and low temperature zone of central Olkaria. He further postulates two possible up-flow zones in Olkaria Northeast and one up-flow zone in Olkaria East, with a down-flow separating Olkaria Northeast and Olkaria East. Extensive boiling also occurs in the up-flow zones to form steam caps below the cap rock. Cold water recharge into the Olkaria geothermal system is assumed to occur from all directions in the 2002 conceptual model. West Japan Engineering Consultants Inc. and subcontractors from 2005 to 2009 (West-JEC, 2009), concluded that the ultimate heat source of the Olkaria geothermal system is considered to be a magma chamber, which has fed the most recent volcanic events in the area. It is further believed that the magma chamber peaks in several locations creating convective heat transfer above these, providing hot recharge to different parts of the geothermal system. This model also proposes up-flows in the Northeast, East and in the Domes sector.

The latest revision of the conceptual model for the Greater Olkaria Geothermal System carried out by Mannvit/ ÍSOR/Vatnaskil/Verkís Consortium (2011), had the following findings:

1) The heat source of the geothermal system is assumed to be a deep-seated magma chamber or chambers. Three main intrusions are believed to extend up from the magma chamber(s) to shallower depths of 6 – 8 km. These heat source bodies (possibly partially molten) are proposed to lie beneath Olkaria Hill (Olkaria West), in the northeast beneath the Gorge Farm volcanic centre, and in the Domes area.

2) Four major geothermal up-flow zones were identified from the temperature and pressure model related to these heat sources. Firstly an up-flow zone feeding the West field seems to be associated with the Olkaria Hill heat source body. Secondly two up-flow zones, one feeding the Northeast field and another feeding the East field and the northwest corner of the Domes, are probably both associated with the heat source body beneath the Gorge Farm volcanic centre. Finally an up-flow zone appears to be associated with the ring structures in the southeast corner of the Domes field, related to the heat source proposed beneath the area. The existence of these up-flow zones was supported by Cl- concentration data and Na/K temperature estimates as well as resistivity data.

3) Permeability of the Olkaria system is mainly controlled by predominantly NW-SE and NE-SW trending faults as well as the proposed ring structure and intersections of such structures. Colder water flows into the system through the N-S fault system along the Ololbutot fault and possibly into the Domes area from the northeast. The Ololbutot fault presents a flow barrier between the eastern and western halves of Olkaria.

## 2. GEOLOGICAL SETTING

The Greater Olkaria volcanic complex, which is located in the African rift, is characterized by numerous volcanic centres of Quaternary age (Macdonald et al., 1987, Marshall et al. 2009). These volcanic centers appear as steep-sided domes formed by successions of lavas and/or pyroclastic rocks, or as thick lava flows of restricted lateral extent. Magmatic activities associated with this complex commenced during the late Pleistocene and continue to recent times

as indicated by the Ololbutot comendite lava, which has been dated at 180±50 yrs B.P (Clarke et al., 1990). It is the only occurrence of surface comendite within the Kenya rift. (Lagat, 2004). Other Quaternary volcanic centres adjacent to Olkaria Volcanic complex include Longonot volcano to the east, Suswa caldera to the south, and the Eburru volcanic complex to the north (Figure 3). Whereas the other volcanoes are associated with calderas of varying sizes, Olkaria volcanic complex does not have a clear caldera subsidence structure. The presence of a ring of volcanic domes in the east, south, and southwest (Figure 3) has been used to invoke the presence of a buried caldera (Naylor, 1972; Virkir, 1980; Clarke et al., 1990; Mungania, 1992). Seismic wave attenuation studies for the whole of the Olkaria area have also indicated an anomaly in an area coinciding with the proposed caldera (Simiyu et al., 1998). Other studies on Olkaria have not identified the existence of the caldera e.g., resistivity studies do not map a clear discontinuity at the margin of the proposed caldera (Onacha, 1993). Ignimbrite flows that could have been associated with the caldera collapse have not been positively identified in Olkaria (Omenda, 1998). Furthermore, petrochemistry of lavas within the Olkaria area shows that they were produced from discrete magma chambers (Omenda, 2000). Another explanation to the caldera hypothesis, which has been proposed, is that the ring structure was formed by magmatic stresses in the Olkaria "magma chamber" with the line of weakness being loci for volcanism (Omenda, 2000).The geological structures (Figure 3) within the Greater Olkaria volcanic complex include; the ring structure, rift fault systems, the Ol"Njorowa gorge, and dykes swarms. The faults are trending ENE-WSW, N-S, NNE-SSW, NW-SE and WNW-ESE. The NW-SE and WNW-ESE faults are thought to be the oldest fault system and they link the parallel rift basins to the main extensional zone (Wheeler and Karson, 1994). Gorge Farm fault is the most prominent of these faults. It bounds the geothermal fields in the north eastern part and extends to the Olkaria Domes area. The most recent structures are the N-S (Ololbuttot eruptive fissure) and the NNE-SSW faults.

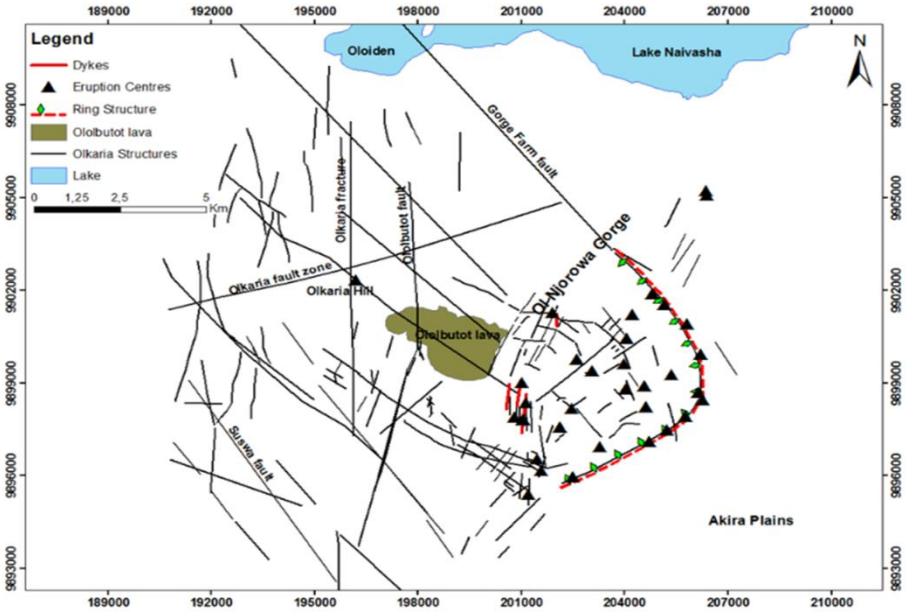


**Figure 3: Updated structural map of the Olkaria volcanic complex (Munyiri 2016)**

## 3 METHODOLOGY

### *3.1 Current model update*

Current model update has incorporated data sets from the newly drilled wells and also more surface exploration data. A new and uniform data analysis boundary has been adapted for geological, geochemical and reservoir engineering data analyses to ensure the datasets are interpreted together with ease of comparative study. More emphasis is placed at joint interpretation of the entire data from the Olkaria field in this update as well as analysis of individual discipline data. A greater effort is also taken to ensure data accuracy and precision before they are input in Petrel software for joint interpretation

### *3.2 Geology*

Relevant geological data were acquired through desktop work and also analytical procedures. Desk top work involved collection of already existing data, borehole location data, surface geological and structural maps and other related information with emphasis on fractures, faults and general tectonic setting, aerial photos and other remote sensing data. Rock cuttings collected at 2 m interval at the drill site, but in cases where the sample were subjected to binocular and petrographic analysis. Binocular analysis was used in noting essential features such as; colour(s) of the cuttings, rock type(s), grain size, rock fabrics, original mineralogy, alteration mineralogy and intensity while petrographic analysis were used to study the mineralogical evolution, confirm the rock type(s), the alteration minerals, and any additional alteration minerals not observed by the binocular microscope. The resulting rock types encountered in a well from the analysis of rock cuttings was used to compile the stratigraphy of the well. Also of importance from the analysis was to note the first appearance of temperature dependent minerals

### *3.3 Geophysics*

The sensitivity of electrical conductivity to the presence of small quantities of interconnected fluids makes the electromagnetic (EM) method particularly applicable to geothermal areas, especially where a water-dominated reservoir is heated by a hot, partially molten magmatic body. Both the water-reservoirs and the magmatic body produce conductive anomalies that can be defined by EM methods. Two sets of data were applied in this analysis, Magnetotelluric (MT) and Transient electromagnetic (TEM) data.

The TEM data) were processed by TemxUSF and TemxZ. TemxUSF is a new version of temx for TerraTEM equipment. The program reads the USF file output of TerraTEM and enables visual edit of data by throwing out the outlier points before the data is used in TEMTD for inversion (Árnason, 2006a). TEMTD program was used for the GOGA data to perform 1D inversion. In 1D inversion it is assumed that the earth consist of horizontal layers with different resistivity and thickness. The program runs on a Linux operation system and can be used for joint inversion of MT and TEM, alone. In case of joint inversion, the program is used to determine the best static shift for MT data and indicate the static shift value hence solve the shift problem.1-D interpretation calculates the layered model and determines where it best fits the measured response.

The MT data analyzed in this paper were acquired by magnetotelluric equipment MTU-5A made by Phoenix geophysics Canada. This processing involves the editing of the parameter file to

reflect the setup of the data acquisition and furrier transform of the resulting time series data to frequency domain. MT editor program was then used to display the phase curves, the apparent resistivity and the cross powers used to calculate each point of the curve. The program was also used to edit or smoothen the data further by removing outliers considered as noisy data points on the phase or apparent resistivity curve. The final result from MT Editor was stored in EDI format (Electromagnetic data interchange) ready for inversion in TEMTD program.

### *3.4 Geochemistry*

The geochemical data presented here comprises of data from wells in Olkaria from various periods of discharge. The data used comprises of water collected at 1 bar absolute in the weir box of the discharging wells. The fluid was sampled through standard sampling procedures for geothermal waters and the samples taken through analysis procedures as described in Arnósson et al. (2006), Arnórsson et al., (2000) and Stefánsson et al., (2007) as described below.

The pH of the water phase was measured on site and samples for the determination of dissolved inorganic carbonate (DIC) were collected into air tight glass bottles for later determination in the laboratory. Samples for $H_2S$ analysis were collected in a similar way for on-site analysis. Samples for determination of major cations including Si, B, Na, K, Mg, Ca, Al, and Fe were filtered through a 0.2 μm pore cellulose acetate membrane into high density polyethylene plastic bottles and acidified to 0.5% using Suprapur$HNO_3$. Samples for F and Cl determination were filtered as described above but not further treated. Samples for $SO_4$ analysis were also filtered as described above, followed by the addition of 2 ml of 0.2 M Zn-acetate in order to precipitate H2S out of solution. A further sample for SiO2 analyses was collected; this sample was not filtered and was diluted on site with deionized water at a 1:10 ratio.

Changes in concentration of components of the reservoir fluid change as the water rises up a geothermal well during discharge. Phase separation occurs by lose of steam and gases from the primary fluid. The sample collected at 1 bar-a was recalculated to the reservoir fluid composition by adding lost steam caused by depressurization boiling as the fluid ascents up a well to discharge in the atmosphere. The reference temperature used in these calculations was obtained from Na-K geothermometer of Giggenbach(1988). In the calculation of reservoir fluid composition, conservation of mass and enthalpy was assumed i.e., adiabatic conditions.

### *3.5 Reservoir*

Physical measurements made in geothermal wells provide the primary information from which the physical properties of geothermal resource can be evaluated. The most important measurements are the temperature, pressure and the mass flow, made either in the well-bore or at the surface. After well completion, geothermal wells are given time to recover from the cooling effect of the drilling fluids and reach equilibrium with the formation. The temperature and pressure recovery behavior is monitored during the heat-up period so as to obtain information on the location of feed zones and the time series which is later analyzed to estimate the natural undisturbed temperature and the initial pressure of the system.

The temperature and pressure data used in this paper were acquired using the Kuster temperature and pressure mechanical gauges which are regularly calibrated to ensure the accuracy of the measured data. The formation temperature and initial pressure were therefore estimated using a

simple and effective method published by Roux et al (1979) based on the Horner time. The basic concept is the straight line relationship on semi logarithmic scale of measured temperature versus the ratio of the Horner time

## 4 RESULTS

### *4.1 Geology*

The general subsurface strata is divided into four main groups as depicted from the analysis of rock cuttings from the wells, where the top most layer comprise of pyroclastics believed to be from the nearby longonot volcano and it is thicker in domes field than in other production fields in the Olkaria geothermal system. The pyroclastic layer overlies a zone dominated by eruptives of rhyolitic composition. underlain by a series of basaltic lavas intercalated with trachytes. Basalts are less viscous hence flow freely hence has was used as marker horizon in delineating and evaluating possible fault structures both surface and buried. Trachytes form the bottom most series of the Olkaria stratigraphy with subordinate basalts and acidic volcanics. The stratas range from plesitocene age to recent where the Olkaria volcanics are < 095 Ma, Olkaria basalts are 1.65 Ma and the trachytes series are 2.1-1.8 Ma (Omenda 2000) Well OW-922 is located at about 2.3 km east from the proposed caldera margin and slightly outside the perimeter of the Olkaria flank. The stratigraphy shown in this well differs significantly from the Olkaria wells with respect to the absence of basalt and reduced abundance of volcanics of rhyolitic composition. This makes correlation with the Olkaria wells difficult with respect to evaluating major faults such as the caldera

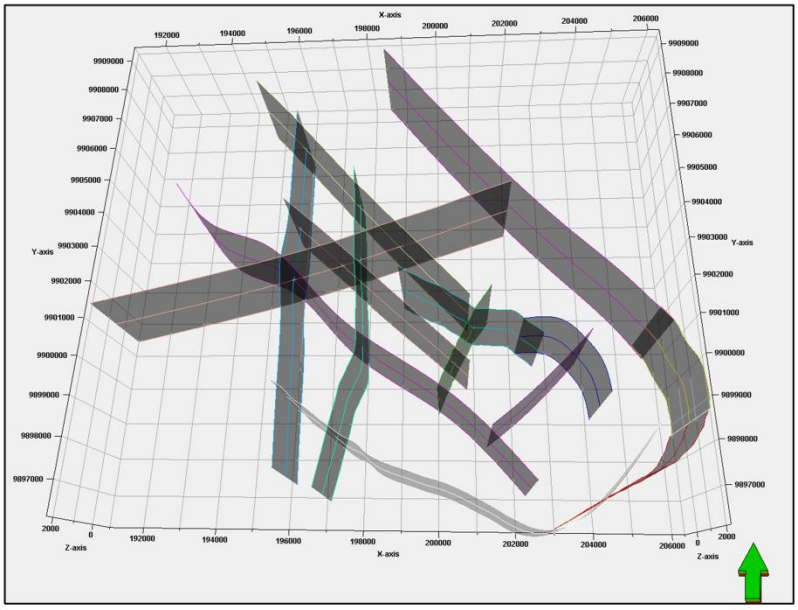


**Figure 4: Major faults assumed to be controlling the Olkaria geothermal system**

Permeability of the Olkaria system is mainly controlled by major faults (Figure 4) predominantly NW-SE, NE-SW and N-S trending faults as well as the proposed ring structure (inner and outer) and intersections of such structures. Both the inner and the outer ring structures connect to the

Gorge Farm fault, located north and east of the main production area. Cooler water is believed to flow into the Olkaria system through the N-S fault system along the Ololbutot fault, which also is associated with plentiful geothermal surface manifestations.

Mapping of intrusions is important in a geothermal system as they can act as conductors of heat into the system and/or permeable zone at the contact with host rock. Intrusions in Olkaria Geothermal system are mainly seen in the lower part of stratigraphy where they occur as sheets or dykes of limited apparent thickness. The intrusives encountered in the stratigraphic analysis include granite, syenite and basalts. Syenite and basalts are observed mainly as dykes and are common in the whole Olkaria production field. Granite appears as a large intrusion encountered at depth in Olkaria East, Southeast and Domes field and apparently becomes dominant below 300 m b.s.l. (~2300 m depth) in the Southeast field.

### *4.1.1 Hydrothermal alteration mineralogy*

The study of hydrothermal alteration mineralogy from drill cuttings during drilling process is key and very important when determining the entrance into the reservoir and the depth of the production casing, interpreting the quantity and type of fluid flowing through the rocks and also in the interpretation of resistivity and magnetic anomaly;. For purposes of this study, it was therefore important to recognize the depth of the upper boundary of temperature dependent alteration minerals. Epidote and actinolite have been considered as they were having more data points and the fact that they were easily identified in binocular analysis making the data more reliable. The upper boundary of epidote (Figure 5) and actinolite (Figure 6) in Olkaria wells has been contoured using Petrel software. Appearance of epidote and actinolite at the upper boundary indicates alteration temperatures of 250°C (Omenda, 1990; Gylfadóttir et al., 2011, Okoo 2013) and 280°C (Lagat, 2007) respectively. The first depth of occurrence of epidote is approximately 1400 m.a.s.l while that actinolite is approximately 1200 m.a.s.l in the Olkaria geothermal field. Various trends in epidote, and actinolite point to structural controls (Figures 5 and 6 ), e.g. near the Ololbutot fault at the central area show shallow high paleo-temperatures while to the south there is a depression in relation to epidote occurrence. Actinolite shows high peaks at the area to the east of Ololbutot fault. Olkaria fault also indicate a hot shallow alteration temperature except in the in the central area in the north east field where both epidote and actinolite appear depressed. The Domes field show a broad elevation of epidote except in the eastern part where it shows a slight depression. A NNE-SSW, NW-SE and W-E elevation trend of actinolite is also evident in the part of domes with a depression around well OW-917. Well OW-922 is a step out well and shows clear indications of depressed hydrothermal alteration. Also of importance to note is the occurrence of smectite, a low temperature clay mineral to total drilled depth in well OW-922. This could indicate that there has been circulation of alkaline and cooler fluids within the proximity of this well for a longer period of geological time.

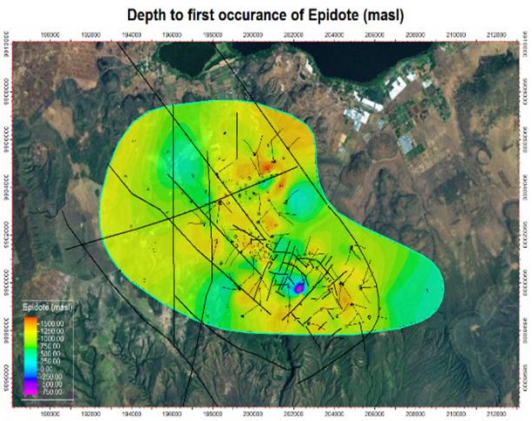


**Figure 5: Distribution of the first occurrence of epidote with faults**

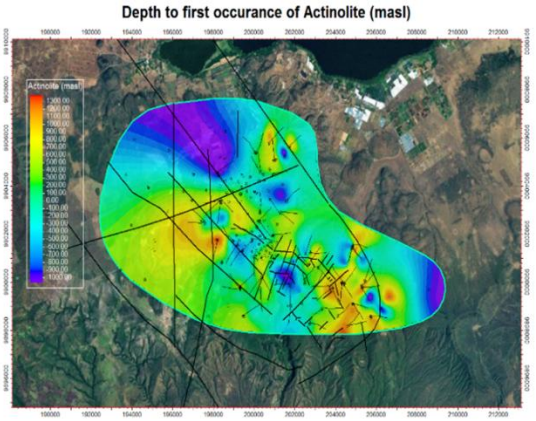


**Figure 6: Distribution of the first occurrence of actinolite with faults**

### *4.1.2 Comparison between alteration and formation temperature*

Alteration is widely used as one way of presenting temperature in a geothermal system, and is assumed to represent the maximum long-term temperature state, while the measured formation temperature represents the present state of the system. A comparison of the two may therefore give indications of the changes that have taken place "recently". Comparison between formation and alteration temperatures (Figures 7 and 8) clearly indicates that the measured formation temperature is far much less than the alteration temperature along the ololbutot in the proximity of OW-39A and at the gorge farm fault around OW-734A. These are probably regions where cooler fluids are

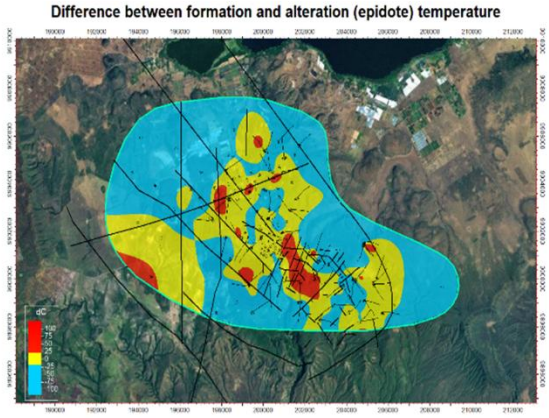


**Figure 7 Comparison of formation and alteration temperature with reference to upper boundary of epidote**

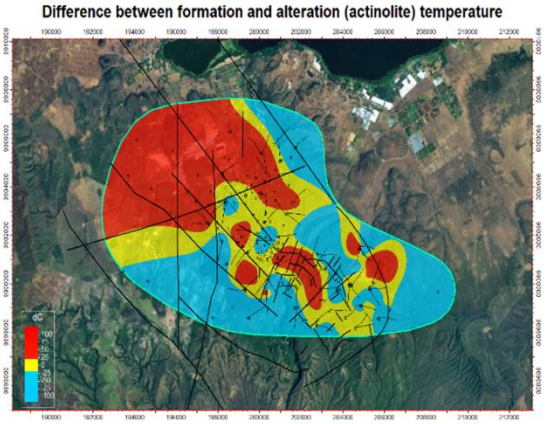


**Figure 8: Comparison of formation and alteration temperature with reference to upper boundary Actinolite**

recharged into the system along these structures. Along the Olkaria fault the contour map show the system within the proximity of the fault is either in equilibrium or heating up except around well OW-731A where some cooling is observed. Several peaks are also observed at the Domes, East, Northeast and in the South East field delineating up-flow zones which could be associated with heat bodies (Figures 7 and 8). In addition, the up flow in the domes that appear to be associated with the ring structures in the east corner of the Domes field could be related to the heat source proposed beneath the Domes area. The field is hotter at depth while at approximately 800 depth most of the field is in either equilibrium or cooling down with a few exceptions. The areas around well OW-922 and the gorge farm fault are cooling down. Alteration and formation temperatures analysis indicate that the cooler fluids flowing through the gorge farm fault and the ololbutot fault are most probably recent.

### *4.2 Geophysics*

Results and interpretations of the joint one-dimensional (1-D) inversion of Magnetotelluric (MT) and central loop Transient Electromagnetic (TEM) data (for static correction of MT) are presented through resistivity iso-maps and cross sections. These inversions were achieved by fitting both data types using the same 1-D resistivity model. The 1-D joint inversion results reveal a resistivity structure with four layered resistivity zones. A shallow superficial high resistivity zone (> 30Ωm) thought to be due to unaltered rock formations and the thick pyroclastic cover is observed across the field. This is succeeded by a thick dome shaped conductive layer (< 6Ωm) that extends to about 200 m.a.s.l in the North West field which thins towards the Central field becoming almost uniform in the South East and the rest of the field. This layer is presumed to be dominated by low temperature alteration minerals such as smectites and zeolites and defines the clay cap. Beneath the base of this conductor is a resistive layer ( >15-50 Ωm) which is thought to be associated with the high temperature secondary minerals such as epidote, chlorite and biotite present in the reservoir. Underlying the resistive layer is another low conductivity layer extending to about 6,000 m.b.s.l which could be associated with the heat source.

#### *4.2.1 1D iso-resistivity maps*

***Resistivity map at 1900 m a.s.****l.*(Figure 9) about 500 m below the ground level shows a resistivity of < 15 Ωm with the western side of the area covered by conductive formation of resistivity < 10 Ωm and the eastern side covered by fairly uniform resistivity of about 10 Ωm covering almost the entire area interpreted to be low temperature alteration minerals like smectite and zeolite formed as a result of hydrothermal alteration fluid filled fractured rock associated with fumaroles.

***Resistivity map at 0 m b.s.l*** (Figure 10) about 2500 m below the ground level. The area is covered by medium to high resistivity (30 – 60Ωm). The high resistivity is seen to cover almost the entire area except western side. The high resistivity is interpreted to be due to the presence of high temperature alteration minerals while medium resistivity is attributed to the presence of low temperature alteration minerals. The increased geophysical survey to the east around OW-922 has revealed more information on the presence of high temperature alteration as is observed at 0 m s.l.

***Resistivity map at 6000 m b.s.l*** (Figure 11), about 8200 m below the ground level, low resistivity anomaly is observed in the whole area but with different intensity. The western side possesses very low resistivity formation which is believed to be due to the influence of heat source below Olkaria hill. The other parts are generally having almost uniform resistivity that is believed to be caused by the presence of heat source underneath domes.

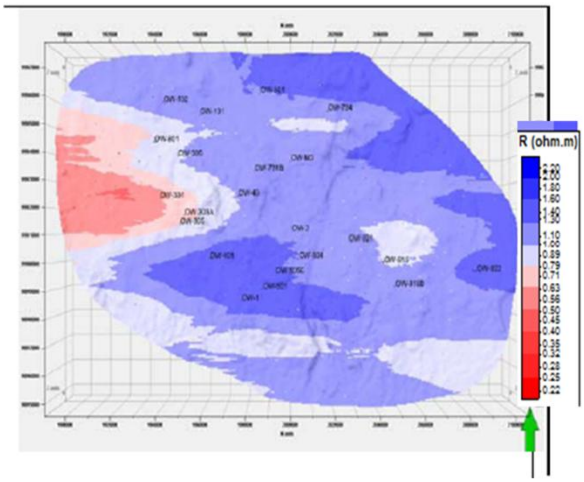


**Figure 9: Iso- resistivity map at 1900 m.a.s.l** depth

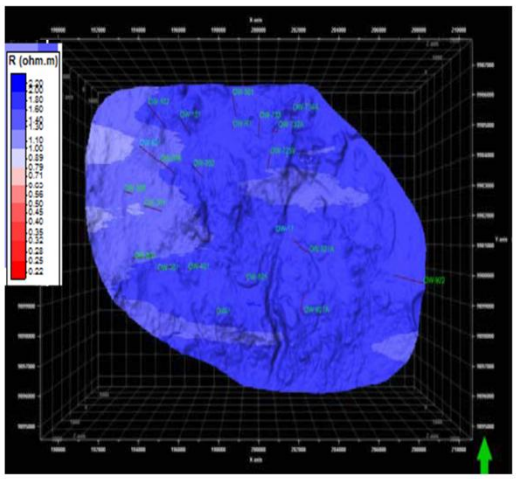


**Figure 10: Iso-resistivity maps at 0 m.a.s.l**

### *4.2.2 1D Cross-Sections (NS moving WE direction)*

**Profile 1** The cross sections (Figure 12) are dissecting the area in N-S direction across the production field of Olkaria. The resistivity structure generally shows a four-layer high-low-high-low resistivity pattern. There is a very good correlation between the resistive anomalies and the most productive wells.

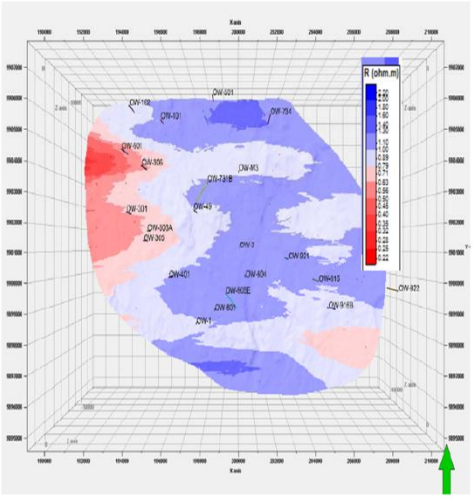


**Figure 11: Iso-resistivity maps at 6000 mbsl**

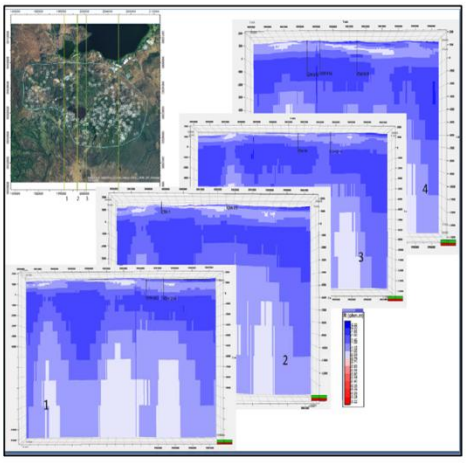


**Figure 12: 1D models along four resistivity profiles running N-S and moving from W-E (Central Field, Domes and North East)**

The deep wells in the Olkaria Domes and Olkaria Central field correspond to the deep high resistivity anomaly defined by MT data, while the low productive wells fall within the generally conductive shallow subsurface layer. The shallow structure reflects the lithological response of shallow formations, which are quite conductive and interpreted to be due to the presence of low temperature alteration minerals. It is clear that the low resistivity cap on the western side is of different composition and is thicker as compared to the low resistivity on the Eastern side. Lack of alteration mineralogy in the drilled wells to the West (Oserian Wells) i.e OW-101 has made it difficult to correlate the alteration mineralogy with resistivity. The alteration mineralogy on the Eastern part of the study area is in agreement with resistivity.

**Profile 2 and 3** The cross sections (Figure13) are running W-E direction covering about 20 km. The resistivity structure generally shows a four-layer high-low-high-low resistivity trend. The high resistivity near surface is uniform along the profile and is associated with the presence of unaltered formations and superficial deposits. This is underlain by a low resistivity which is not uniform along the profile. The western side possesses a highly conductive and probably much more conductive than the Illitic clays and other high temperature mineralization that occur above 200°C therefore, in most high temperature geothermal systems. There is a characteristic clay "cap" that forms above the main high temperature reservoir and often on the sides of geothermal systems, particularly in outflow areas. This clay cap is readily the most dominant feature observed in the resistivity surveys and thus provides a useful indicator of the location and extent of the underlying high temperature reservoir. The base of the clay cap usually marks the transition to high temperature reservoir while the top marks the upper extent of thermal activity (about 50°C). The clay cap layer to the western side is thicker than the clay cap to the eastern side which might mean change in the casing design and depth of drilling to accommodate the high temperature zone.

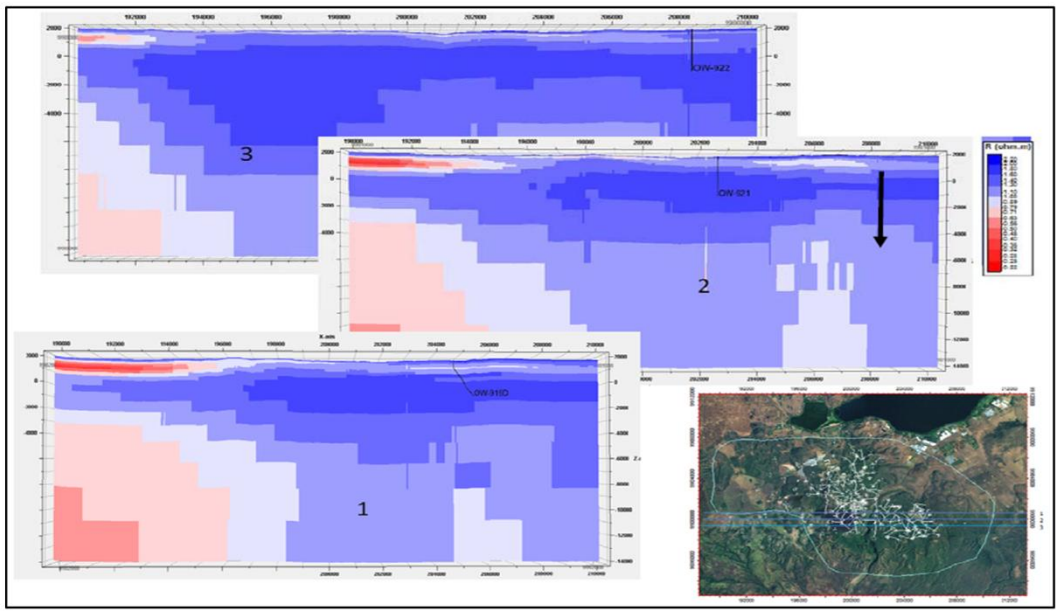


**Figure 13: 1-D models along three resistivity profiles running W-E and moving from N-S**

## 4.3 Geochemistry

### *4.3.1 Reservoir fluid composition*

Olkaria geothermal field wells discharge two phase. Two phase fluid results from boiling of reservoir fluid as the pressure is lowered during the ascent of the fluid. Boiling results into portioning of components dissolved in the fluid into the water phase and the steam phase depending on if the component is volatile or non-volatile Volatile components e.g. the non-acidic gases ($CH_4$, $N_2$, $H_2$) will partition wholly into the vapour phase while the non-volatile components (mostly cations and anions) remain in the water phase. For the purposes of interpretation of geothermal reservoir processes, the two phases have to be combined so as to give the chemical composition of the parent one phase fluid.

### *4.3.2 Olkaria well chemistry*

The Cl-$HCO_3$-$SO_4$ ternary diagram can be used to evaluate the extent of geothermal reservoirs. It can be used to locate up flow zones in a geothermal field as well as show recharge zones. The water chemistry discharged from Olkaria wells has a pH of between 5-10 pH units. Recalculated in situ pH is usually between 6.5-7.0 pH units (Karingithi *et al* 2010). The reservoir fluid in Olkaria East field (EPF) and South East (SE) field is composed of mature chloride waters, mostly with the dominant ions being Na and Chloride (Na-Cl water). The wells in the central part of EPF and SE field indicate geothermal waters that characterize the up-flow zones with exception of a few well along the ololbutot fault (due to recharge) which indicate waters found in the peripheral zones. In the NEPF the wells drilled along the Olkaria fault are indicative of mature waters but to the east of the field the wells begin to show indications of $CO_2$ additions to a small extent. Olkaria domes show indicatives of both Na-Cl (up flow zones) and Bicarbonate waters. The bicarbonate water is from the influence of recharge into the system from the fractures in the Ol-Njorowa gorge area to the west of Domes, the Gorge farm fault to the North East and the ring structure to the south east of the Domes field.

The water is of mixed type and majorly comprise of Na-Cl waters typical of high temperature geothermal fields especially in the East and Southeast fields. A mixture of Na–$HCO_3$ or Na–Cl–$HCO_3$ types is also seen in the field mixture of Na–$HCO_3$ or Na–Cl–$HCO_3$ types is also seen in the field in the periphery of the geothermal system.

### *4.3.3 Fluid chloride content and Sodium-Potassium (TNaK) Geothermometer*

Figures 14 and 15 show the chloride distribution and TNaK geothermometer respectively. Cl-ion does not readily take part in formation of alteration minerals and once added in the fluid, the ion remains in solution. The more the water-rock interaction, the higher the Cl ion content. There is relationship between the Cl ion content in the fluid and the calculated NA-K geothermometer. Wells with high Cl fluid have high geothermometer temperatures. However geothermometers are prone to errors that may arise from analytical errors, dilutions and re-equilibration among others as the fluid ascents in the up-flow geothermal reservoirs. Higher formation temperatures in the reservoir correspond with increases in geothermometer temperatures and the Cl ion content of the fluid. It can be said with confidence that chloride is a useful tracer for showing the flow patterns and the extents of the Olkaria Geothermal area as a whole. It also shows the size of the up flow zones and the structures that control the fluid movement for recharge and the up flow.

Na-K geothermometers temperature indicate 250-310°C for Northeast field, 240-320°C for East field, 200-320°C for Domes field and 290-320°C for Southeast field.

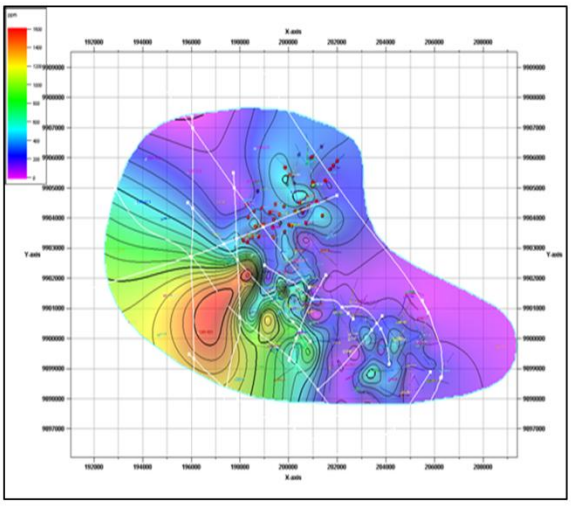

**Figure 14: Chloride concentration distribution for the Olkaria Geothermal field**

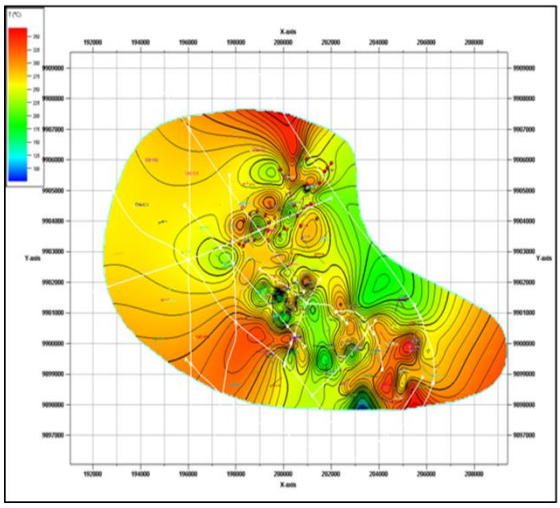

**Figure 15: Sodium –Potassium (TNaK) geothermometer temperature in Olkaria Geothermal Field**

### *4.4 Reservoir*

#### *4.4.1 Reservoir pressure models*

The initial pressure is modelled and presented in this section in a series of horizontal sections cutting through the reservoir at intervals of 250 m from 750 m below the ground level. In the shallow depths at 1400 m.a.s.l, pressure is fairly low (Figure 16) and to some extend isobaric distribution across the field Some few spots however show slightly elevated pressures in the regions dominated by higher temperatures at these depths. At sea level (Figure 17) changes appear to reflect increase in pressure with depth while maintaining similar spatial distribution.

#### *4.4.2 Temperature model*

The temperature distribution at 900 m depth shows a high temperature anomaly which is the location of the up-flow zones associated with the West, Northeast (NEF), East (EF) and Domes fields. The cold recharge along the Ololbutot fault reaches below 0 m a.s.l. as indicated by the temperature of wells OW-201, OW-203, OW-401 and OW-39A. A colder area south of the Olkaria fault in the NEF could indicate cold inflow. At sea level, lower temperatures (Figure 18) are also observed near wells OW-734A and OW-918A cutting across the gorge farm fault and at well OW-922 which is 2 km from the proposed caldera. At 0 m.a.s.l. these low temperature anomalies may indicate these structures (ololbutot fault and gorge farm fault) form part of recharge in the Olkaria system. In the planar sections, the hot area cover broadens but the boundary is not clear. Below 2km depth much hotter structures begin to show in the field probably getting closer to the tops of heated bodies in the subsurface and eventually near the bottom of the model, they unify into a single extremely heated body. A cross section traversing W-E (Figure 19) shows up flows in SEPF and in domes with gradual cooling evident in the East

of Domes. The two up flows are separated by the gorge which clearly appears a possible recharge area.

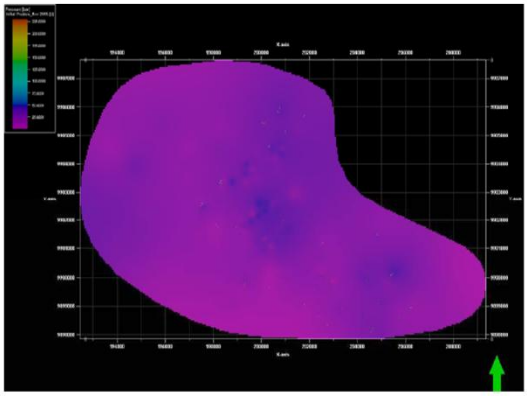

**Figure 16: Pressure at 1450 m.a.s.l.**

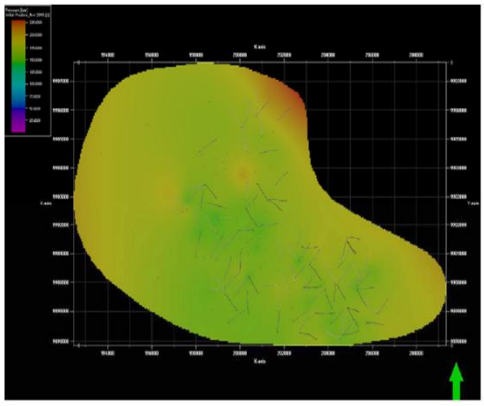

**Figure 17: Pressure at sea level**

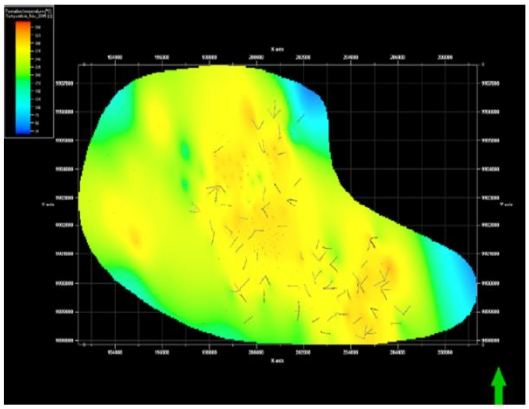

**Figure 18: Temperature at sea level m depth**

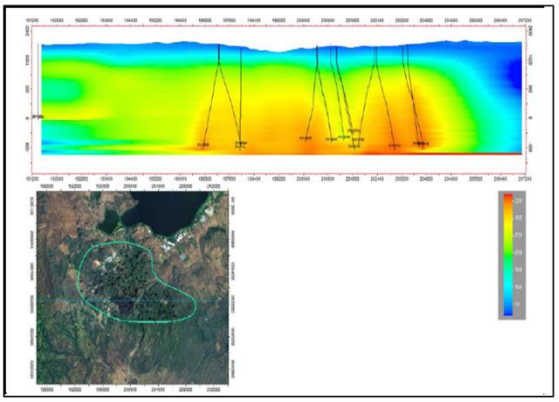

**Figure 19: E-W Formation temperature profile 13**

## 5 CONCLUSION AND THE UPDATED CONCEPTUAL MODEL

### *5.1 Conclusion*

The heat source of the Greater Olkaria Geothermal System is assumed to be a deep-seated magma chamber or chambers. Three main intrusions are believed to extend up from the magma to shallower depths of 6 – 8 km. These heat source bodies (possibly partially molten) are proposed to lie beneath Olkaria Hill (Olkaria West), in the northeast beneath the Gorge farm volcanic centre, and in the Domes area.

Six major geothermal up-flow zones are identified from the comparison between formation temperature and alteration. These up-flow zones appear to be related to the heat sources.

Firstly an up-flow zone feeding the West field seems to be associated with the Olkaria Hill heat source body. Secondly two up-flow zones, one feeding the Northeast field and another feeding the East field and the northwest corner of the Domes, are probably both associated with the heat source body beneath the Gorge Farm volcanic centre. Finally an up-flow zone appears to be associated with the ring structures in the southeast corner of the Domes field, related to the heat source proposed beneath the Domes area. The up flow regions are located under the EPF, NEPF, DPF, WPF, SEPF and the region of OW-101 (CPF and NWPF).

The existence of these up-flow zones is supported by Cl-ion concentration data and Na/K temperature estimates as well as resistivity data. Newly available data from deep wells in the East field, which have elevated Cl concentrations. These high Cl concentrations often, but not always, appear to be correlated with high Na/K and formation temperatures.

Permeability of the Olkaria system is mainly controlled by predominantly NW-SE and NE-SW trending faults as well as the proposed ring structure and intersections of such structures.

The resource distribution is on a NW-SE tend which follows the main strike of hot structures. The intersection of these faults and those carrying the recharge fluids (often strike opposite) such as the N-S Ololbutot and NE-SW Olkaria fault, and others in the southeast often creates plausible conditions for convective reservoirs. This grid faulting is evident in the north east, south east and east fields.

Recharge to the field follows known structural trends water is assumed to flow into the system through the N-S fault system along the Ololbutot and the gorge farm fault (Figure 20) possibly into the Domes area from the northeast. The Ololbutot fault is believed to present a flow barrier between the eastern and western halves of Olkaria, even though indications have appeared of high-temperature resources at great depth in that region.

### *5.2 The conceptual model*

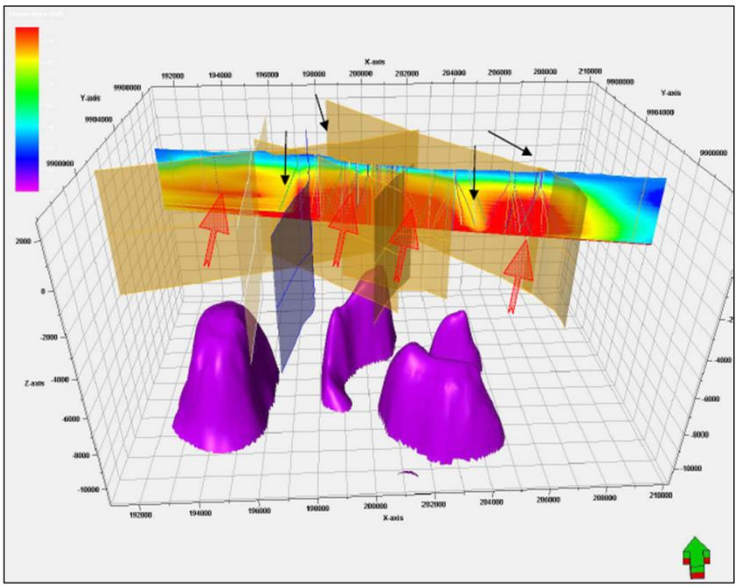

**Figure 20: The updated conceptual model of Olkaria**

## REFERENCES


Arnórsson, S., 2000: Assessment of reservoir fluid composition from wet steam well data. In: Arnórsson,S.(ed.), *Isotopic and chemical techniques in geothermal exploration, development and use. Sampling methods, data handling, interpretation*. International Atomic Energy Agency, Vienna, 241- 266.

Árnason, K., 2006a. TEMTD, *a programme for 1-D inversion of central-loop TEM and MT data. Short manual.* Iceland GeoSurvey - ISOR, internal report, 17 pp.

Arnórsson, S., Bjarnason, J.Ö., Giroud, N., Gunnarsson, I., and Stefánsson, A., 2006: Sampling and analysis of geothermal fluids. Geofluids, 6, 203-216

Clarke, M.C.G., Woodhall, D.G., Allen, D., and Darling G., 1990: Geological, volcanological and hydrogeological controls on the occurrence of geothermal activity in the area surrounding Lake Naivasha, Kenya, with coloured 1:100 000 geological maps. Ministry of Energy, Nairobi, 138 pp.

Giggenbach, W.F., 1988: Geothermal solute equilibria. Derivation of Na-K-Mg-Cageoindicators. *Geochim. Cosmochim. Acta, 52*, 2749-2765.

Axelsson, G., Gudmundsdóttir, V., Arnaldsson, A., Ármannsson, H., Árnason, K., Einarsson, G.M., Franzson, H., Halldórsdóttir, S., Hersir, G.P., Kamunya, K., Koech, V., Mbith, U., Mwarania, F., Nielsson, S., Okoo, J., Ouma, P., Óskarsson, F., Rop, E., and Wamalwa R., 2016A Revision of the Conceptual Model for Olkaria Geothermal System. *Proceedings of the 42nd Workshop on Geothermal Reservoir Engineering, Stanford University, Stanford Carlifornia, 2017*

Gylfadóttir, S.S., Halldórsdóttir, S., Arnaldsson, A., Ármannsson, H., Árnason, K., Axelsson, G., Einarsson, G.M., Franzson, H., Fridriksson, Th., Gudlaugsson, S.Th., Gudmundsson, G., Hersir, G.P., Mortensen, A.K. and Thordarson, S., 2011: *Revision of the conceptual model of the Greater Olkaria geothermal system-phase I.*Mannvit/ÍSOR/Vatnaskil/Verkís Consortium, report, Reykjavík, 100 pp.

Karingithi, C.W., Arnórsson, S., and Grönvold, K., 2010: Processes controlling aquifer fluid compositions in the Olkaria geothermal system, Kenya. *J. Volc. Geothermal Res.*

KenGen 2017: *Mvuke News magazine Issue 4.* April 2017.

Lagat, J.K., 2004: *Geology, hydrothermal alteration and fluid inclusion studies of Olkaria domes geothermal field, Kenya.* University of Iceland, MSc thesis, UNU-GTP, Iceland, report 2, 71 pp.

Lagat, J., 2007: *Borehole geology of OW-904A*. KenGen, Kenya, internal report.

MacDonald, R., Davies, G.R., Bliss, C.M., Leat, P.T., Bailey, D.K., and Smith, R.L., 1987: Geochemistry of high silica peralkaline rhyolites, Naivasha, Kenya rift valley. *J. Petrology, 28*, 979-1008.

Marshall, A. S. l., Macdonald R., Rogers N. W., Fitton. J. G., Tindle, A. G. N., Nejbert, K., and Khinton, R. W., 2009: Fractionation of peralkaline silicic magmas: The Greater Olkaria volcanic complex, Kenya Rift valley.*J. Petrol., 50,*323-359.

Mungania, J., 1992: *Preliminary field report on geology of Olkaria volcanic complex with emphasis on Domes area field investigations*. Kenya Power Company, internal report.

Naylor, W.I. 1972: *The geology of Eburru and Olkaria geothermal prospects*. UNDP project report, KPC, 58 pp.

Ofwona, C.O., 2002: A reservoir study of Olkaria East geothermal system, Kenya. MSc thesis, University of Iceland and United Nations University Geothermal Training Programme, UNU-GTP report 1 – 2002, Reykjavík, 74 pp.

Okoo, J.A., 2013: Borehole geology and hydrothermal alteration mineralogy of well OW-39A, Olkaria geothermal project, Naivasha, Kenya. Report no 24 in: *Geothermal training in Iceland* 547-576

Omenda, P.A., 1998: The geology and structural controls of the Olkaria geothermal system, Kenya. *Geothermics, 27-1,* 55-74.

Omenda, P.A., 2000: Anatectic origin for comendite in Olkaria geothermal field, Kenya Rift; Geochemical evidence for syeniticprotholith. *African J. Science and Technology. Science and Engineering Series, 1*, 39-47.

Omenda P.A and Simiyu S., 2015: Country update report for Kenya 2010-2014. *Proceedings of the World Geothermal Congress 2015, Melbourne Australia,* 11pp

Onacha, S.A., 1993: Resistivity studies of the Olkaria-Domes geothermal project. Kenya Power Company, internal report.

Simiyu, S.M., Oduong, E.O., and Mboya, T.K., 1998: *Shear wave attenuation beneath the Olkaria volcanic field.* KenGen, Kenya, internal report, 29 pp

Stefánsson, A., Arnórsson, S and Bjarnason, J.Ö., 2007: Fluid-fluid interaction in geothermal systems. Reviews in Mineralogy & Geochemistry, 65, 229-312.

SWECO and Virkir, 1976: *Feasibility report for the Olkaria geothermal project*. Report prepared for The United Nations and Government of Kenya.

Wheeler, W.H., and Karson, J.A., 1994: Extension and subsidence adjacent to a ‘‘weak’’ continental transform: an example of the Rukwa Rift, East Africa. *Geology, 22,* 625-628.

Virkir Consulting Group, 1980: *Geothermal development at Olkaria*. Report prepared for Kenya Power Company.

West-JEC, 2009: The Olkaria Optimization Study (Phase II) – Final reservoir analysis report. West Japan Engineering Consultants, Inc., 301pp.